Transport pathways of carbon monoxide from Indonesian fire pollution to a subtropical high-altitude mountain site in western North Pacific

Saginela Ravindra Babu[1*], Chang-Feng Ou-Yang[1], Stephen M. Griffith[1], Shantanu Kumar Pani[1], Steven Soon-Kai Kong[1], and Neng-Huei Lin[1,2*]

[1]Department of Atmospheric Sciences, National Central University, Taoyuan 32001, Taiwan.

[2]Center for Environmental Monitoring and Technology, National Central University, Taoyuan 32001, Taiwan.

Correspondence to**:** S. Ravindra Babu (baburavindra595@gmail.com) and Neng-Huei Lin (nhlin@cc.ncu.edu.tw).

Abstract: Dry conditions associated with El Niño and a positive Indian Ocean Dipole (IOD) are known to have caused major fire pollution events and intense carbon emissions over a vast spatial expanse of Indonesia in October 2006 and 2015. During these two events, a substantial increase in carbon monoxide (CO) mixing ratio was detected by in-situ measurements at Lulin Atmospheric Background Station (LABS, 23.47°N 120.87°E, 2,862 m ASL) in Taiwan, the only background station in the subtropical western North Pacific region. Compared to the long-term October mean (2006-2021), CO was elevated by ~47.2 ppb (37.2%) and ~36.7 ppb (28.9%) in October 2006 and 2015, respectively. This study delineates plausible pathways for CO transport from Indonesia to LABS using MOPITT CO observations and MERRA-2 reanalysis products (winds and geopotential height (GpH)). Two simultaneously occurring transport pathways were identified: (i) horizontal transport in the free troposphere and (ii) vertical transport through the Hadley circulation (HC). The GpH analysis of both events revealed the presence of a high-pressure anticyclone over the northern part of the South China Sea (SCS), which played an important role in the free tropospheric horizontal transport of CO. In this scenario, CO in the free troposphere is transported on the western edge of the high-pressure system and then driven by subtropical westerlies to LABS. Simultaneously, uplifted CO over Indonesia can enter the HC and transfer to subtropical locations such as LABS. The vertical cross-section of MOPITT CO and MERRA-2 vertical pressure velocity supported the transport of CO through the HC. Further, the results revealed a distinct HC strength in two events (higher in 2006 compared to 2015) due to the

different El Niño conditions. Overall, the present findings can provide some insights into understanding the regional transport of pollution over Southeast Asia and the role of climate conditions on transport pathways.

Keywords: Indonesian fire pollution; Carbon monoxide; Lulin Atmospheric Background Station; Hadley circulation

1. Introduction

Fire activity over Southeast Asia (SEA), particularly over the Maritime Continent (MC, including Indonesia), is a severe environmental problem that causes widespread regional pollution in the lower troposphere and impacts atmospheric chemistry, air quality, and climate at regional to global scales. Over the MC, fires occur predominately in the dry season (August to October) and particularly during the periods of drought, often associated with the positive phase of El Niño-Southern Oscillation (ENSO) events (Duncan et al., 2003a; van der Werf et al.,2008, 2017; Field et al., 2009, 2016). A recent study has also highlighted the role of the Indian Ocean Dipole on MC fire activity (Pan et al., 2018). For example, dry conditions associated with the positive IOD during the 2015/16 El Niño and 2006/07 El Niño events led to increased fire activity over Indonesia and the wider MC (van der Werf et al.,2008; Chandra et al., 2009; Nassar et al., 2009; Huijnen et al., 2016; Field et al., 2016). Due to these intense fires, an enormous amount of carbon emissions was released into the atmosphere in the form of carbon dioxide (CO_2), carbon monoxide (CO), and methane (CH_4) (Huijnen et al., 2016; Field et al., 2016; Parker et al., 2016; Heymann et al., 2017). The impact of these two Indonesian fire events on carbon emissions, tropospheric trace gases, aerosol composition, and air quality has been extensively discussed in the literature (Chandra et al., 2006; Logan et al., 2008; Chandra et al., 2009; Nassar et al., 2009; Huijnen et al., 2016; Field et al., 2016; Heymann et al., 2017; Ravindra Babu et al., 2019). For example, the fire carbon emissions during September-October 2015 over Maritime SEA were the largest since 1997 (Huijnen et al., 2016). By using Greenhouse gases Observing SATellite (GOSAT) data, Parker et al. (2016) reported the strong enhancement of CO_2 and CH_4 over the Indonesian region.

CO is a significant emission from the combustion of fossil fuels and biomass (forest and savanna fires, biofuel use, and waste burning) and is widely used as a tropospheric tracer for these sources (Ou-Yang et al., 2014; Pani et al., 2019). Inter-annual variability of CO in the tropics and

sub-tropics is largely linked to year-by-year changes in biomass burning (BB) emissions. Indonesian fires often emit large quantities of CO by incomplete combustion associated with the occurrence of peat fire pollution. Although CO is not a direct greenhouse gas (GHG), it does have a global warming potential due to its chemical reactions in the atmosphere. CO is also an ozone (O_3) precursor in the troposphere, and indirectly increases radiative forcing (0.23 +/- 0.05 W m^{-2}) through the production of O_3 and CO_2 and depletion of hydroxyl radical, the primary chemical reactant with CH_4 in the atmosphere (IPCC, 2013). The lifetime of CO in the free troposphere is ~ two months, thus can be a tracer from polluted upwind regions to remote downwind areas (Cooper et al., 2012). Some of the studies reported the influence of Indonesian fire activity and the transport of CO from Indonesia to the Indian Ocean, Southern Pacific, and western Pacific Ocean (Matsueda and Inoue, 1999; Pochanart and Akimoto, 2003; Nara et al., 2011; Matsueda et al., 2002, 2019). However, the underlying transport mechanisms sending this fire pollution to downwind northern hemisphere subtropical locations, particularly transport to high-altitude background locations in the western north Pacific are still unclear.

Taiwan is located downwind of East Asia and Southeast Asia, which are major air pollutant source regions. As result, Lulin Atmospheric Background Station (LABS, 23.47°N 120.87°E, 2862 m above sea level), was constructed in 2006 to study the transboundary transport of these air pollutants and their impact on Taiwan. LABS is not affected by local sources, i.e., industrial and traffic emissions, making it an ideal site for measuring long-range transport of air pollutants, complementing the global network of the Global Atmospheric Watch (GAW) in the East Asia region where no other high-altitude background station is available (Ou-Yang et al., 2014, 2022). In the framework of Seven South-East Asian Studies (7-SEAS, Reid, et al., 2013; Lin et al., 2013; Wang et al., 2015), several studies at LABS have reported on the long-range transport of northern peninsular Southeast Asia (PSEA) BB pollutants to Taiwan through the low-level jet (LLJ) and the related impacts on air quality and chemistry over Taiwan (Ou-Yang et al., 2012, 2014; Lin et al., 2013; Chuang et al., 2016; Chi et al., 2016; Tsay et al., 2016; Hsiao et al., 2016; Lin et al., 2017; Park et al., 2019; Pani et al., 2016, 2019; Huang et al., 2019; Huang et al., 2020; Ravindra Babu et al., 2022). However, to date, no studies have shown the potential influence of Indonesian fire activities on LABS measurements and the BB pollution from Indonesian fires reaching LABS. Surprisingly, the extensive fire events in 2006 and 2015 allowed us to track CO concentrations from the Indonesian peat fires to LABS in Taiwan. By combining in-situ and satellite CO

measurements and large-scale circulation parameters from reanalysis products, we identified plausible transport pathways from Indonesia to LABS.

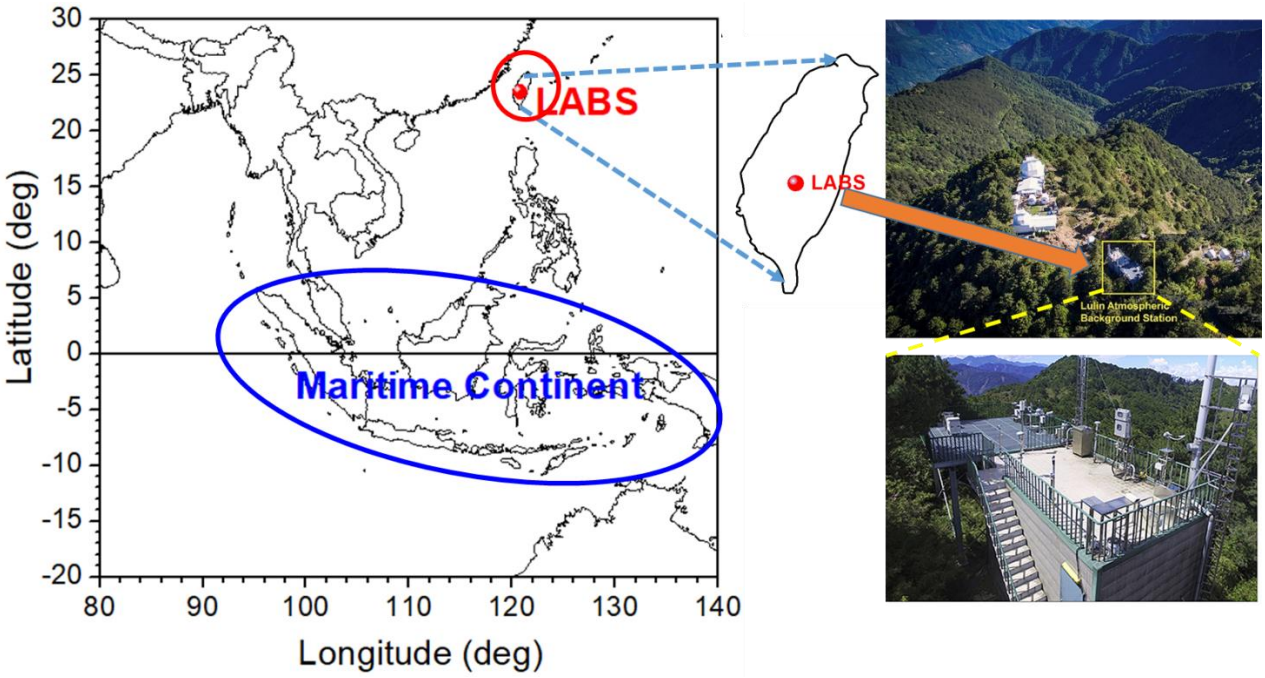

Figure 1. Geographic location of the Maritime Continent and Lulin Atmospheric Background Station (LABS, 23.47°N 120.87°E, 2862 m ASL), Taiwan.

2. Site description, data and methodology

2.1 Site description

LABS is located on the summit of Mount Lulin and is shown in Figure 1, along with the location of the Maritime Continent. Hiking is the only way to access LABS, taking about 30 minutes from the nearest parking lot. There are no known point emission sources at the summit or in the surrounding area with the exception of the occasional maintenance activity at the Lulin Observatory. Because of the high altitude of LABS, measurements there are not affected by local pollution from factories, traffic, and other domestic sources; rather, it is strategically located to monitor long-range transported air pollutants from the Asian continent. More details about the instruments and their specifications can be found in Sheu et al., 2009.

2.2 In-situ measurements

Details of the CO and various meteorological measurements at LABS employed in the current study have been previously described in detail (Sheu et al., 2009; Ou-Yang et al., 2014; Ravindra Babu et al., 2022) and are thus only briefly described here. The long-term monthly mean of various meteorological parameters such as temperature, relative humidity, wind speed, and wind direction along with CO at LABS can be found in **Sup. Figure 1**. The overall mean temperature (relative humidity) was about 10.5^{o}C (~80%), with monthly mean temperatures ranging between ~5 and 14^{o}C. Local wind direction is mostly from the southwest and to a lesser extent from the northeast. Long-term monthly mean in CO shows distinct seasonal patterns with a springtime maximum and a summertime minimum at LABS. CO measurements were measured by a nondispersive infrared (NDIR) analyzer (APMA-360, Horiba, Japan) at LABS. Hourly averages of the 6-s data were analyzed in this study. The detection limit of the NDIR is ~20 ppb (1σ) (Zellweger et al., 2009); more details about CO measured at LABS can be found in Ou-Yang et. (2014). The magnitude of the CO concentration enhancement in 2006 and 2015 above the long-term background was determined by comparing a 16-year average (2006-2021) of October CO data at LABS. We obtained the percentage change in CO relative to the respective background using Equation 1:

$$\text{Relative change in percentage} = \left(\frac{x_{i-\bar{x}}}{\bar{x}}\right) \times 100 \qquad \text{(Eq. 1)}$$

where x_i represents the monthly mean of October in 2006 and 2015, and $\bar{x}$ is the corresponding monthly long-term mean calculated using the data from 2006 to 2021 (Ou-Yang et al., 2014).

2.3 Satellite measurements

CO observations from the Measurement of Pollution in the Troposphere (MOPITT, version 8) instrument were also utilized in this study (Worden et al., 2010; Deeter et al., 2019). MOPITT is a multi-channel Thermal InfraRed (TIR) and Near InfraRed (NIR) instrument operating onboard the sun-synchronous polar-orbiting NASA Terra satellite. V8 CO products, consisting of a CO profile at ten pressure levels, have been validated; more details about the retrieval algorithm, validation, and uncertainties of MOPITT CO can be found in Deeter et al. (2019). In addition to the MOPITT measurements, we utilized CO from the Atmospheric Infrared Sounder (AIRS) on the NASA Aqua satellite, which provides CO at different vertical levels twice daily and near-

global coverage. AIRS uses wavenumbers 2,183-2,200 cm^{-1} (4.58-4.5 μm) for retrieving CO (McMillan et al., 2005). Version 8, level 3 CO product, available at 1° ×1° resolution at various pressure levels, was utilized in the present study. AIRS data were downloaded from the following website https://disc.gsfc.nasa.gov/datasets/AIRS3STM_7.0 (AIRS project., 2019). AIRS sensitivity to CO is broad and optimal in the mid-troposphere between approximately 300 and 600 hPa (Warner et al., 2007; Warner et al., 2013; AIRS project., 2019). CO retrievals have a bias of 6-10% between 900 hPa and 300 hPa with a root mean square error of 8-12 % (McMillan et al., 2011).

Apart from MOPITT and AIRS CO data, we used Moderate Resolution Imaging Spectroradiometer (MODIS) collection 6.1 daily active fire hot spot data from 2006–2021 over Indonesia (Giglio et al., 2016).

2.3 MERRA-2 Reanalysis products

We also utilized monthly mean geopotential height (GPH), wind vectors (zonal and meridional wind speed), and pressure vertical velocity from the Modern-Era Retrospective Analysis for Research and Applications, version 2 (MERRA-2). MERRA-2 is the latest atmospheric reanalysis data produced by the NASA Global Modeling and Assimilation Office (GMAO) (Gelaro et al., 2017). The horizontal resolution of MERRA-2 reanalysis is $0.5^{o} \times 0.625^{o}$. MERRA-2 data are available online through the NASA Goddard Earth Sciences Data Information Services Center (GES DISC; https://disc.gsfc.nasa.gov/, last access: 11 September 2022).

3. Results and Discussion

3.1 Higher CO mixing ratios in October 2006 and 2015 over Maritime Continent and at LABS

Figure 2 shows the height-time cross-section of monthly mean CO over the Maritime Continent (MC) obtained from MOPITT and AIRS from 2003 to 2021. There is a significant inter-annual variability in the CO time series in **Figure 2** as observed by both instruments. The maximum CO mixing ratio for this time period was observed in the fall of 2006 and 2015; both were tied to El Niño events (Field et al., 2016; Ravindra Babu et al., 2019). Several studies have reported on the impact of the intense fire activity in 2006 and 2015 and on the release of significant carbon emissions and poor air quality over the wider Equatorial Asia region (Logan et al., 2008; Chandra

et al., 2009; Field et al., 2016; Huijnen et al., 2016; Ravindra Babu et al., 2019). Even though 2009 and 2014 were El Niño years, the CO over MC was not as high as observed in 2006 and 2015. The weaker and shorter duration of fire activities could largely explain the lower CO over the MC in 2009 and 2014 in contrast to those in 2006 and 2015. Furthermore, **Figure 3** shows the temporal variability of monthly mean CO from MOPITT and AIRS from January through December in both years 2006 and 2015, respectively. Both instruments show maximum CO enhancement in October compared to the remaining months in 2006 and 2015. Overall, it is clear from **Figures 2** and **3** that in October 2006 and 2015, CO over the Maritime Continent in the entire troposphere increased dramatically due to increased CO emissions near the surface from extreme fire activity (**Fig. 4c**).

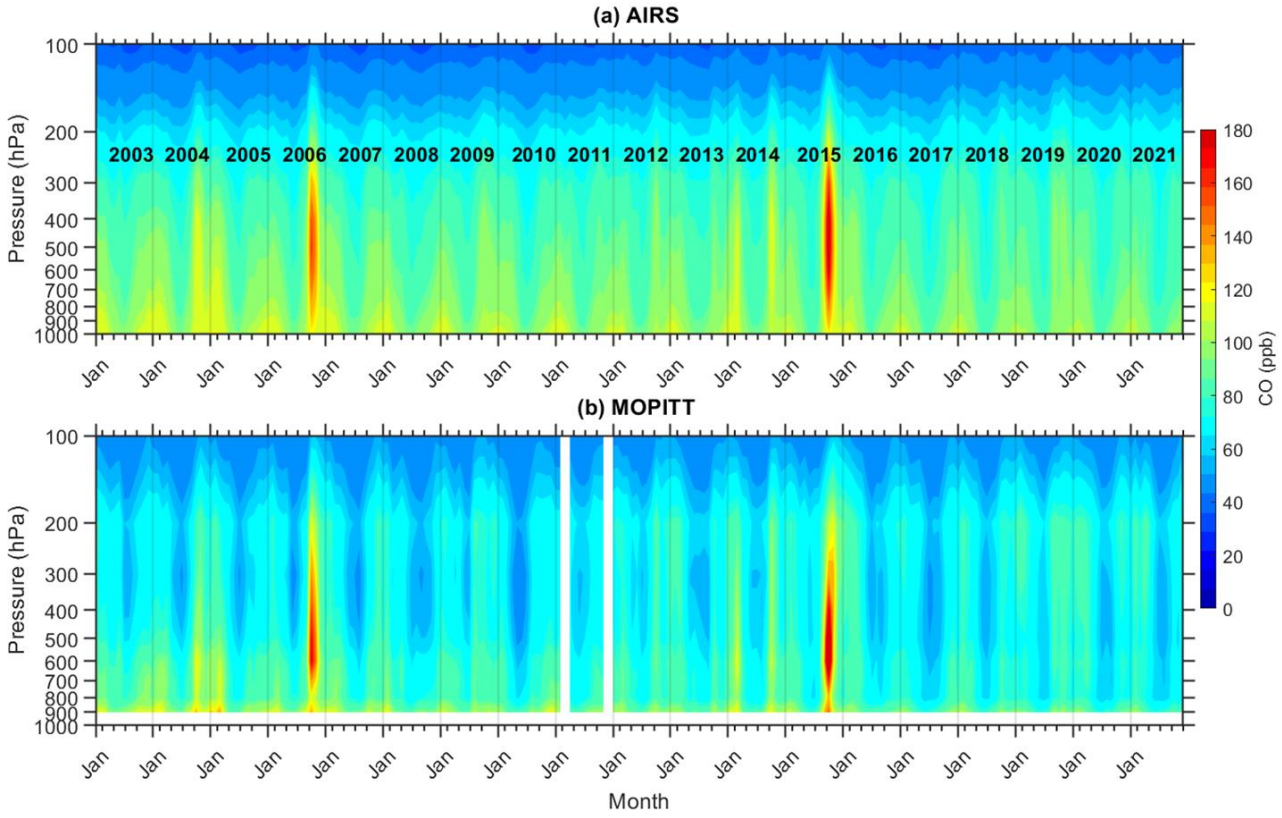

Figure 2. Pressure-time cross-section of monthly mean carbon monoxide observed over the Maritime continent (average over 90E-140E,10S-10N) during 2003-2021 obtained from (a) AIRS, and (b) MOPITT satellite measurements.

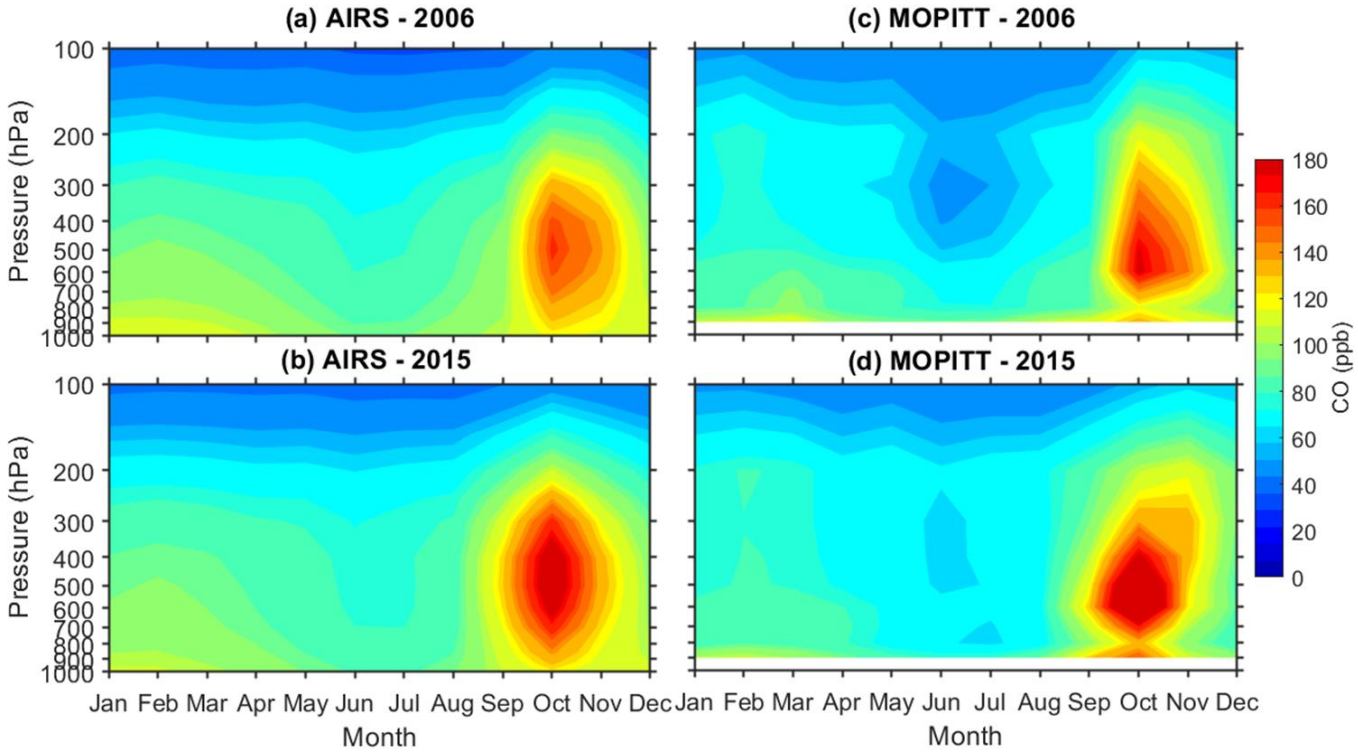

Figure 3. Pressure-time cross-section of monthly mean carbon monoxide observed over the Maritime continent (average over 90E-140E,10S-10N) in (a) 2006, (b) 2015 obtain from AIRS satellite measurements. Subplots (c) and (d) are the same as subplots (a) and (b) but for the MOPITT satellite measurements.

Figure 4 summarizes the inter-annual variations of CO in October observed at LABS along with MODIS active fire counts over Indonesia and the observed Niño 3.4 and the IOD index values, which helped to motivate this study. The highest CO mixing ratios for this period were observed in 2006 and 2015, well over the long-term means of 132.1±23.3ppb when including all points and 126.8±19.6 ppb when excluding 2006 and 2015. A significant enhancement of CO, over the latter mean calculation, of more than 47.2 ppb (37.2%) in 2006 and 36.7 ppb (28.9%) in 2015 was observed, with the value in 2006 (2015) more significant than the ±2σ (±1σ) standard deviation of the long-term mean (**Table 1**). Higher CO mixing ratios in 2006 and 2015 at LABS were also evident from the MOPITT and AIRS satellite measurements obtained over a 1-degree radius around the LABS location (Sup. **Fig. 1**).

Unprecedented CO values in 2006 and 2015 at LABS could be due to the transport of CO from large-scale forest fires that were intense during the same period in the Indonesian region. It

is clear from **Figure 4**, that the higher values of CO at LABS in 2006 and 2015 coincided with more intense fire activity over Indonesia along with warm phases of ENSO and IOD (**Fig. 4c and 4d**), which have been extensively studied due to the induced drought conditions in those years (Field et al., 2016; Huijnen et al., 2016; Pan et al., 2018). Previous studies (e.g., Logan et al., 2008; Zhang et al., 2011; Field et al., 2016; Pan et al., 2018) have demonstrated the direct relationship between strong Indonesian fires and El Niño events. . The enhanced CO values from the 2006 and 2015 events at LABS in the present study complement the findings of Matsueda and Inoue (1999) in the case the of 1997 El Niño event and Nara et al. (2011) in the case of 2006 El Niño event. However, the impact on CO at LABS occurred significantly further north of the source region than in either of the aforementioned studies. Based on aircraft measurements, Matsueda and Inoue (1999) reported the enhancement of CO_2, CO, and CH_4 in the upper troposphere (at 9-12 km) over the South China Sea (SCS) during October 1997 Indonesian fire event. However, this large CO increase appeared only over the SCS west of Kalimantan and not in the subtropics between 10^oN and 26^oN. Nara et al. (2011) reported a substantial increase in CO mixing ratios over the Western Tropical Pacific Ocean (between 15^oN and the Equator) by shipboard observations routinely operated between Japan and Australia and New Zealand during October and November of 2006. Similarly, Pochanart and Akimoto (2003) also reported the influence of the 1997 Indonesian fire event on CO enhancement at the rural station Srinakarin (14°220N, 99°070E, 296 m above sea level) in Thailand.

In addition, due to La Niña and the negative phase IOD, the fire activity in Indonesia during 2016 was much less intense than in 2006 and 2015 (**Fig. 4c** and **4d**). Interestingly, CO at LABS during 2016 exhibited the lowest October values in the entire data period, ~39.8 ppb (31.4%) lower than the long-term October mean (2006-2021). It is well known that the major sources of CO at LABS are BB from peninsular SEA in spring and industrial emissions from continental Asia in winter (Ou-Yang et al., 2014; Pani et al., 2019; Ravindra Babu et al., 2022; Ou-Yang et al., 2022). However, October is a transition month from the summer to winter at LABS, when air masses can still arrive from the Pacific Ocean. Our analysis (**Fig. 4**) suggests that the extensive fires that occurred during the 2006 and 2015 El Niño events over Indonesia may have yielded the unprecedented CO mixing ratios at LABS in October of those years. Combined El Niño and IOD-related changes in the large-scale dynamics and circulations may have promoted CO emissions from Indonesian fires to transport to LABS.

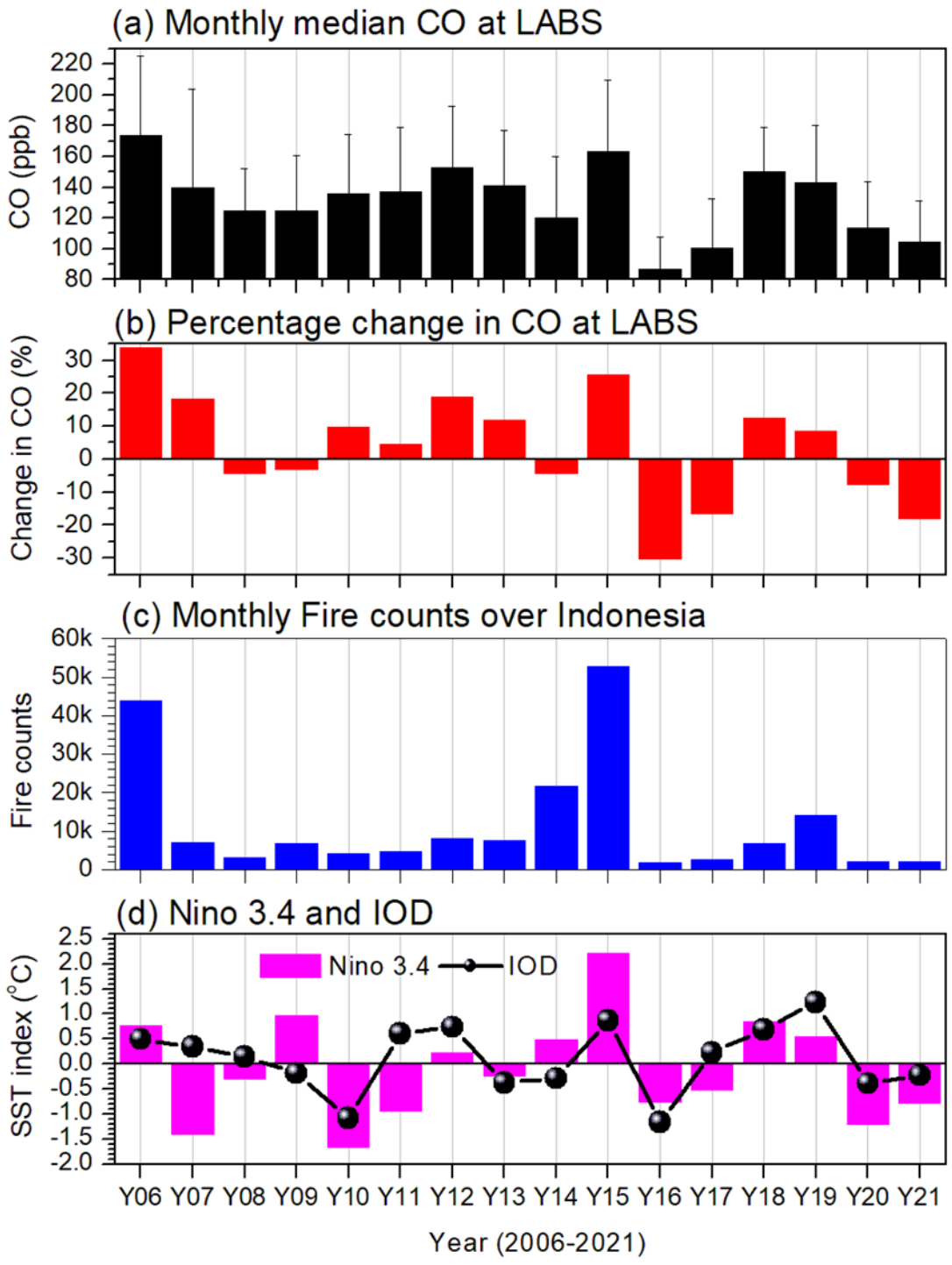

227

228 **Figure 4.** Inter-annual variations in October of the (a) monthly median of CO, (b) percentage
229 change in CO from the long-term mean at LABS, (c) MODIS (Moderate Resolution Imaging
230 Spectroradiometer) total active fire counts (only fires tagged with >30 % confidence) over

Indonesia, (d) sea surface temperature index for Niño 3.4 (magenta) and Indian ocean dipole (black) during 2006 to 2021.

To confirm the impact of Indonesian fire pollution on LABS CO, we further checked the spatial distribution of CO in 2006 and 2015 from the MOPITT satellite CO observations. An inter-comparison between October monthly mean CO at LABS (2006-2021) and MOPITT and AIRS CO data at 700 hPa within the 1-degree radius around the LABS location yielded correlation coefficients of 0.88 and 0.78 ($p<0.01$), respectively (Sup. **Fig. 2**). We then used the MOPITT satellite data to track the spatial and vertical CO changes in October 2006 and 2015; first, we examined the distribution of the CO anomalies at free tropospheric heights in those years. **Figure 5** shows these anomalies compared to the long-term mean (2001-2021) at 700 hPa and 500 hPa, revealing extensive enhancements of CO mixing ratios over most of equatorial Asia in 2006 and 2015. **Figure 5** indicates that CO from the Indonesian fires affected both the Indian Ocean to the west and South Pacific and the northern Pacific to the east. Furthermore, these outflows of CO split northwestward into the Bay of Bengal and northeastward into the western North Pacific. It is also worth noting that the anomalies were significantly higher at 500 hPa than 700 hPa. Elevated CO is visible in the Taiwan region at 700 hPa and 500 hPa in both years. This further provides a clear signature of the impact of Indonesian fire activity on enhanced CO in 2006 and 2015 at LABS. Overall, from **Figure 5**, MOPITT CO data shows the Indonesia fires transported CO vertically and horizontally in all directions. We further investigated the associated dynamics and large-scale circulations supporting the transport of Indonesian pollution to LABS.

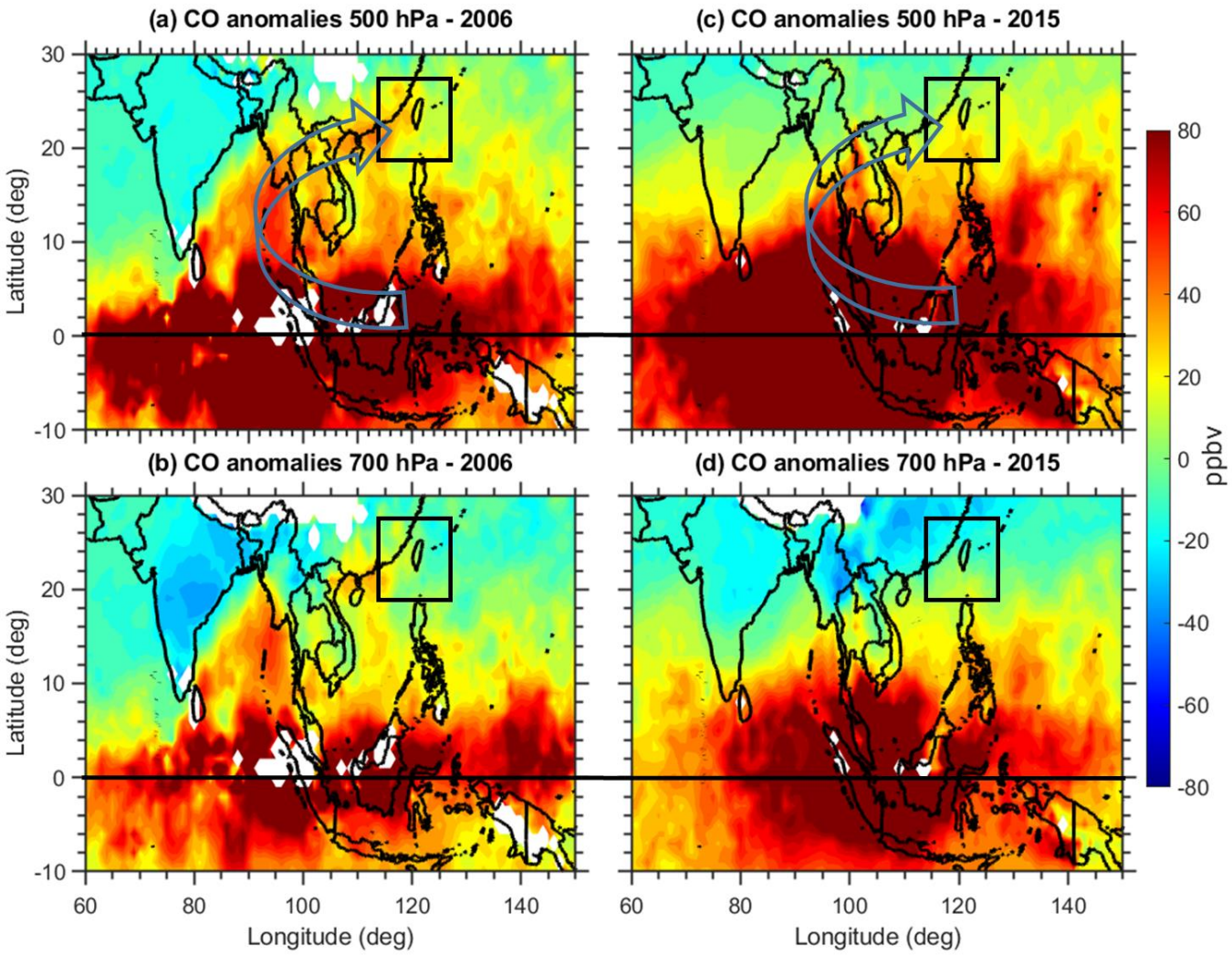

Figure 5. Monthly mean CO anomalies obtained from MOPITT satellite observations (a) at 500 hPa and (b) at 700 hPa during October 2006. Subplots (c) and (d) are the same as subplots (a) and (b) but for October 2015, respectively. The anomalies are obtained by subtracting the 2006 and 2015 data from the long-term mean of MOPITT CO data from 2001 to 2021.

3.2 Role of large-scale dynamics and atmospheric circulations

Large-scale dynamics and circulations can play a crucial role in transporting Indonesian pollution to long-distance downwind regions (Bowman, 2006; Nara et al., 2011; Matsueda et al., 2019). To understand the plausible mechanisms behind the transport of Indonesian fire pollution to LABS, we further examined the MERRA-2 reanalysis of geopotential height (GpH) and wind distribution in 2006 and 2015. The spatial distribution of GPH at two pressure levels (700 and 500 hPa) in both events is shown in **Figure 6**. The GpH and wind vectors in the two event years

exhibited quite different patterns in relation to a high-pressure system over the northern parts of the SCS. A high-pressure anti-cyclonic circulation center extended from the Indo-China Peninsula to the SCS in October 2006 with LABS located precisely on the eastern edge of the anticyclone. In 2015, the anticyclone extended from the Indo-China Peninsula to the western North Pacific region and over Taiwan.

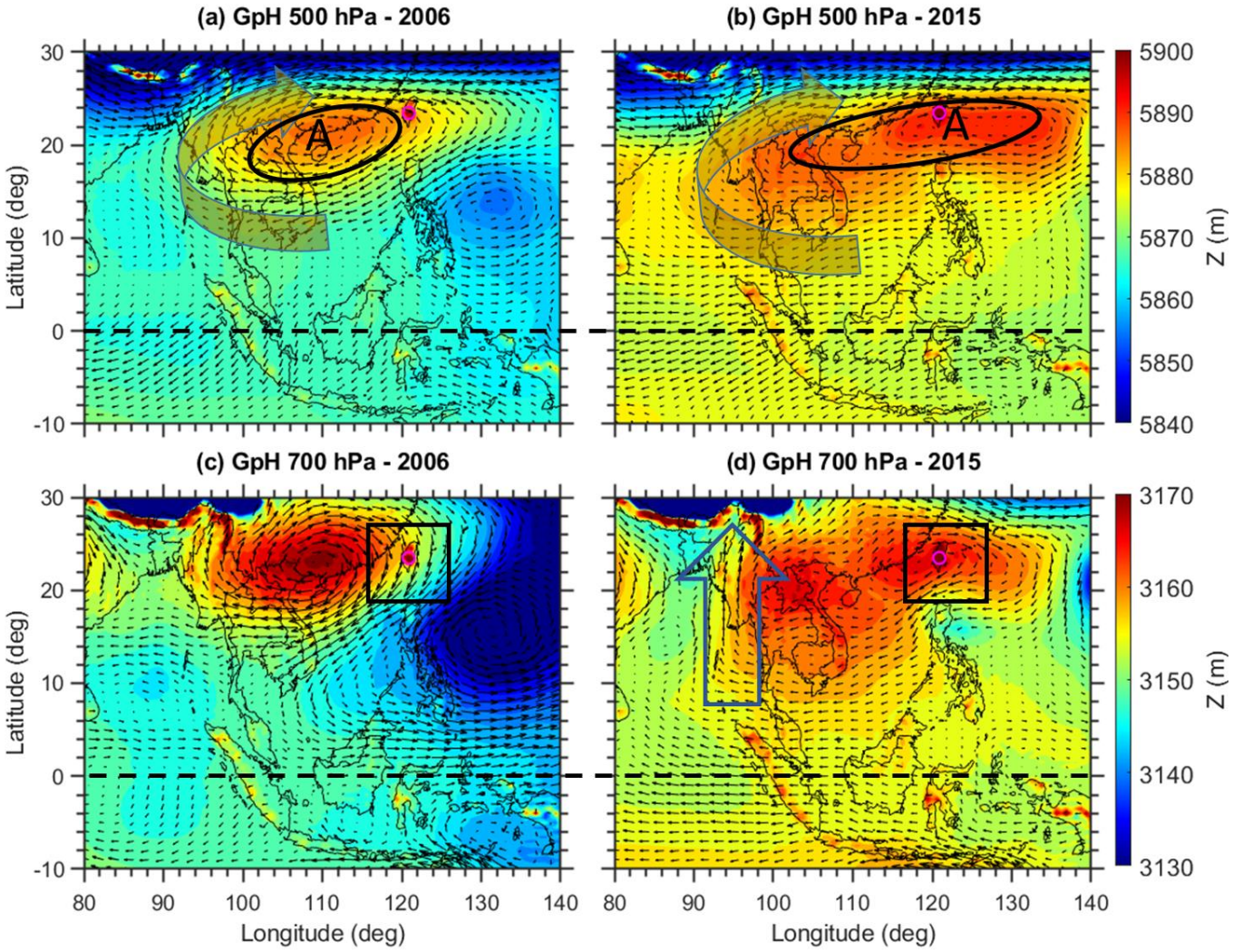

Figure 6. Monthly mean Geopotential height (GpH) obtained from MERRA-2 reanalysis (a) at 500 hPa and (b) at 700 hPa during October 2006. Subplots (c) and (d) are the same as subplots (a) and (b) but for October 2015.

During both event years, strong southerlies at 500 hPa were evident due to the high-pressure anticyclone system in the northern SCS. It is assumed that the northern edge of the Indonesian fire pollution plume can be carried out by the southerlies and around the western edge

of the high-pressure anti-cyclone over SCS. An apparent merging of the southerlies from the equator with the subtropical westerlies in the northern PSEA region subsequently led to the transport of CO to downwind LABS. Overall, in both events, there was a significant anticyclone over the SCS. El Niño and the positive IOD-induced high-pressure anticyclone over SCS strengthen the southerlies from the equator, consequently bringing higher amounts of CO to LABS. We further investigated the vertical pressure velocity (omega) behavior in both events (Sup. Fig 3**)**, where negative (positive) values represent upward (downward) winds. Significant upward wind in both events was evident over equatorial MC, while vertical pressure velocity over Taiwan and surrounding regions at both pressure levels were mostly downwards in 2006 and 2015. The presence of a downwind will provide downward transport of any pollutant presence in the upper troposphere over that region. Also, the downward wind was relatively higher in 2006 compared to 2015. The center of the downward wind was shifted eastwards in the western North Pacific in 2015. The distinct behavior of vertical pressure velocity around LABS during these two events might be due to the associated climate conditions in the two periods; more discussion will be provided in section 3.4.

We further showed CO deviations at both pressure levels in October 2016 when there was very low fire activity in Indonesia (**Fig. 8**). Interestingly, there was a significant lowering of CO over the Taiwan region in 2016, which agrees with the observed low CO values from the in-situ measurements at LABS **(Fig. 4b)**. Also in agreement, 2016 was a La Niña and negative IOD year and fire activity was much weaker (**Fig. 4c** and **4d**). During the La Niña years, large-scale dynamical processes are greatly reversed with respect to El Niño years. We further analyzed the GpH and wind circulation patterns in 2016 (**Fig. 9)**. A significant high-pressure system (western North Pacific subtropical High) was present over the western North Pacific region in 2016, which was shifted considerably further eastward compared to the SCS in 2006 and 2015. The wind vectors also highlighted the transport of a clean marine air mass from the Pacific Ocean to LABS in 2016. Interestingly, the vertical pressure velocity exhibited a pronounced upward wind over Taiwan in 2016, in contrast to the downward wind in 2006 and 2015. This indicates that dominant clean marine air reached LABS in 2016 resulting in the lowest CO mixing ratio in the entire dataset at LABS.

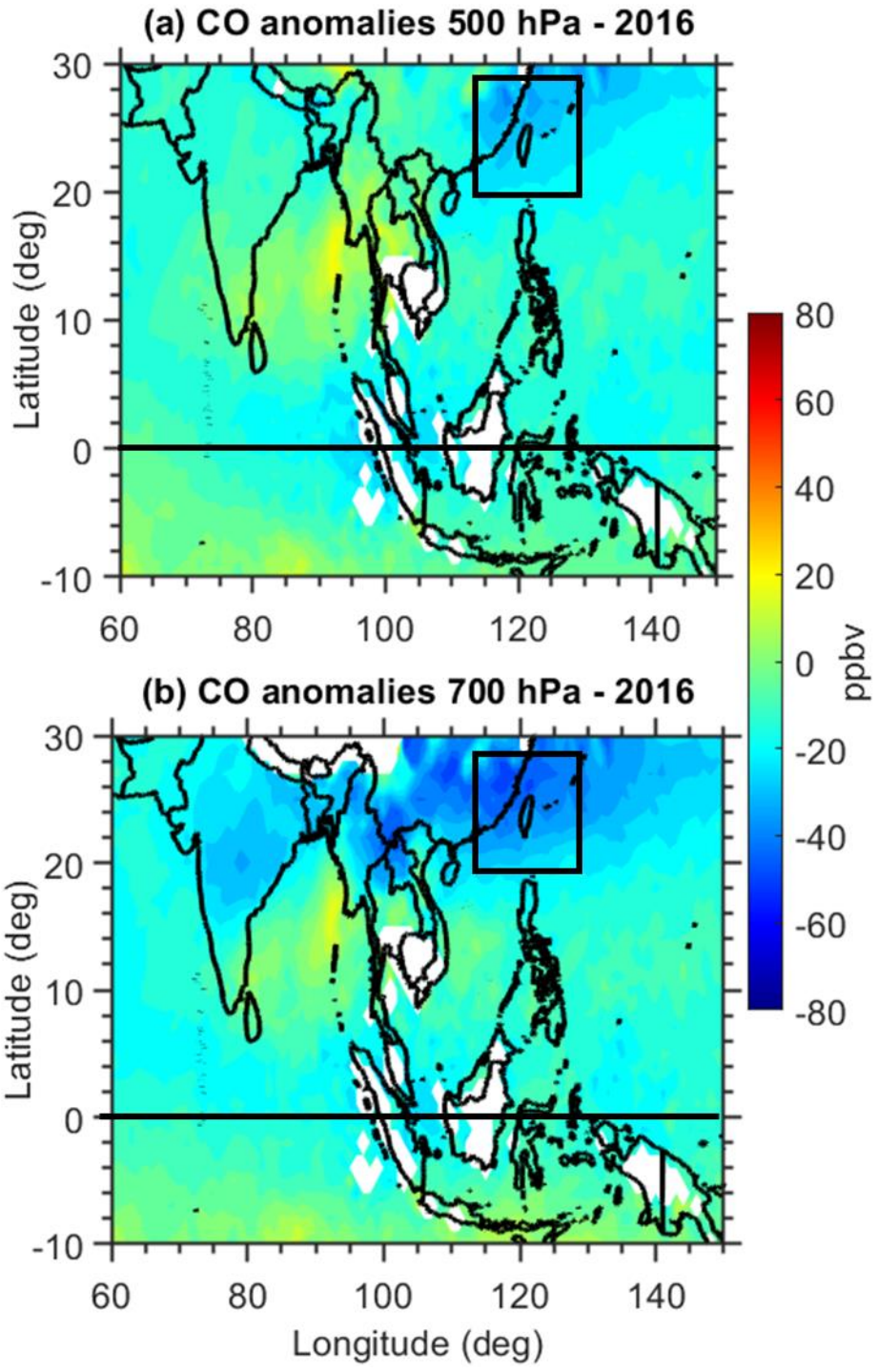

304

305 **Figure 8.** Monthly mean CO deviations from the long-term mean (2001-2021) were obtained
306 from MOPITT satellite observations (a) at 500 hPa and (b) at 700 hPa during October 2016.

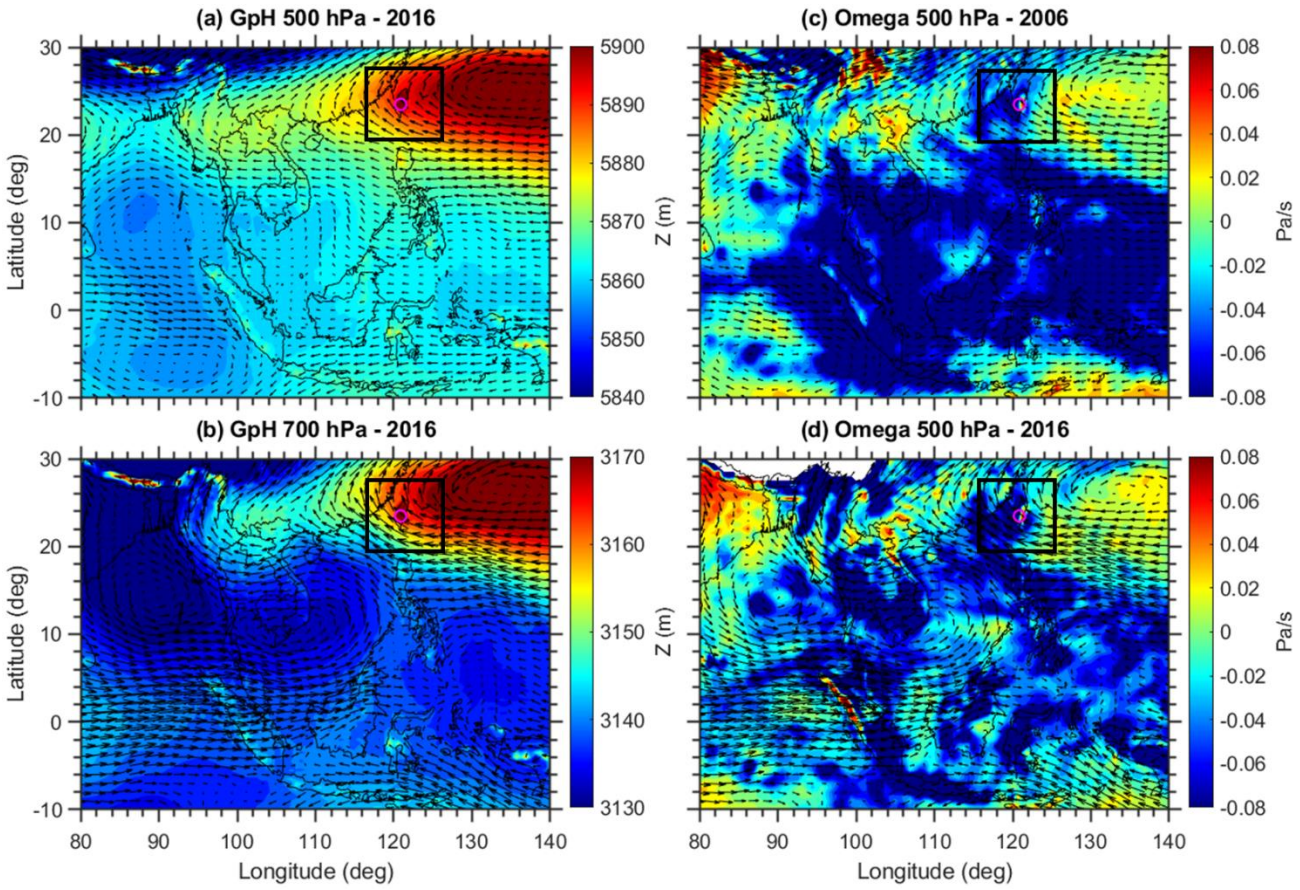

Figure 9. Monthly mean Geopotential height (GpH) obtained from MERRA-2 reanalysis (a) at 500 hPa, and (b) at 700 hPa during October 2016. The subplots (c) and (d) are the same as subplots (a) and (b) but for the observed vertical pressure velocity (Omega).

3.4 Role of Hadley circulation

The Hadley circulation (HC) is a crucial component of the climate system, which is characterized by a thermally driven large-scale meridional circulation (Hadley, 1735). This circulation links the troposphere and stratosphere and the tropics and extra-tropics, through horizontal and vertical motions, transporting moisture, heat, and momentum to regulate Earth's energy budget. As the CO sources (Indonesia) in this study were close to the equator, the air is expected to rise more or less directly over the CO sources. **Figure 10** shows the vertical-meridional cross-section of CO and vertical pressure velocity in separate panels averaged along 110°–130°E in October 2006 and 2015. The black-colored vertical line in all the panels in **Figure 10** shows the location of LABS and the horizontal line represents the 700 hPa. The vertical cross-section of CO highlights the uplifting of CO into the upper troposphere over the equator, followed by southward

and northward movement in both 2006 and 2015 (**Fig. 10a** and **10b**). A clear transport of CO from the source region to the sub-tropics via meridional transport was evident in both events. It is noted that the higher CO observed between 20–30°N latitude below ~700 hPa is related to anthropogenic emissions and not due to the Indonesian fires. To confirm the lofted CO from Indonesia really descended in the subtropics due to the Hadley circulation, we looked into the vertical cross-section of vertical pressure velocity in both events. From **Figure 10**, it is suggested that large amounts of CO from Indonesia were transferred into the free troposphere by the strong upward air motion in this region. Similarly, there was a pronounced descending motion (positive values of vertical pressure velocity) during October 2006 (**Fig. 10c**) in the northern hemisphere subtropics around 20–30°N latitude, which corresponds well with the location of LABS. However, in October 2015, the descending motion was not significant compared to 2006. This may be due to the different El Niño conditions in 2006 and 2015. While IOD conditions were indeed similar between 2006 and 2015 (**Fig. 4d**), the higher descending motions in 2006 can be explained in part by the moderate El Niño conditions during that year. A well-developed El Niño condition was already established in 2015 compared to 2006. In October 2006, the observed Niño 3.4 value was around 0.7 whereas in 2015 it was around 2.21. These values indicate that the El Niño conditions were already well established in October 2015 whereas, in 2006, the conditions were not developed as El Niño. It is reported that in El Niño conditions, the western Pacific HC is observed to be weakened whereas the eastern Pacific HC is strengthened (Wang, 2004). This is supported by the observed lesser descending motions in 2015 from the present study. These differences in the descending motions likely influenced the greater CO enhancement in 2006 compared to 2015 at LABS (**Fig. 4b** and **Table 1**). Overall, it is clearly illustrated from the MOPITT CO vertical cross-section and the MERRA-2 vertical pressure velocity that the CO emitted from the Indonesian fire was transported vertically through the Hadley circulation to the LABS location.

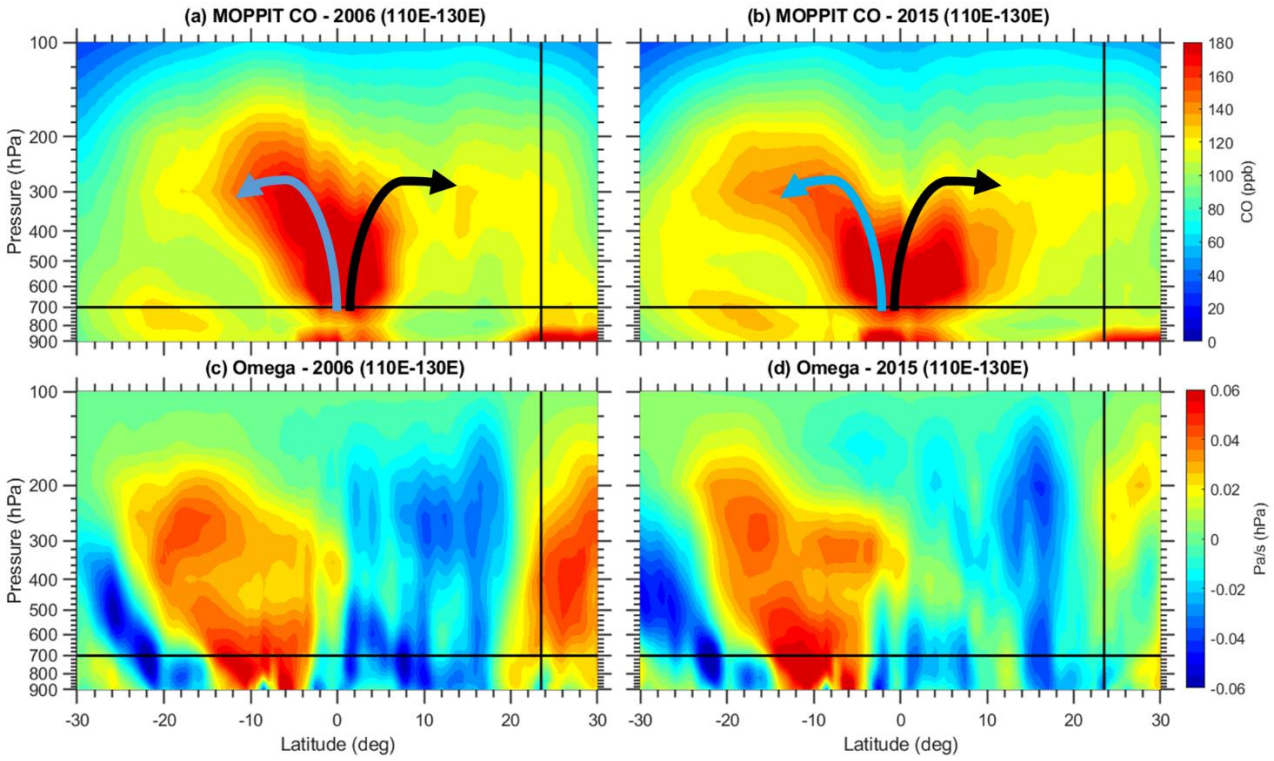

Figure 10. Pressure–latitude cross-section of MOPITT CO averaged along 110°–130°E (a) for October 2006 and (b) for October 2015. Subplots (c) and (d) are the same as subplots (a) and (b) but for the MERRA-2 reanalysis vertical pressure velocity. Positive (negative) values represent the downward (upward) wind.

One of the worst fire events in Indonesia's history occurred in October 1997 and was associated with an El Niño event and a positive IOD (Duncan et al., 2003a). In order to see any similarities between 1997 and 2006 and 2015, particularly in large-scale circulations, we further checked the MERRA-2 GpH and wind circulation pattern in October 1997. To note, none of the satellite measurements of CO (either AIRS or MOPITT) are available during the 1997 event, and measurements at LABS didn't start until 2006. Hence, we only cross-checked the large-scale circulations that are observed in October 1997, respectively. Sup. Figure 4a shows the spatial distribution of GpH observed at 500 hPa and Sup. Figure 4b shows the vertical-meridional cross-section of vertical pressure velocity averaged along 110°–130°E in October 1997. Interestingly, we noticed a significant high-pressure anti-cyclonic circulation over northern parts of the SCS in October 1997 as observed in 2006 and 2015. Also evident is the merging of the southerlies from the MC with the subtropical westerlies in the northern PSEA region. Similarly, the vertical

pressure velocity also shows the upward wind over the MC and the downward wind over the northern hemisphere subtropics around 20–30°N latitude. From Sup. Figure 4b, it is very clear that a significant descending wind was evident around the LABS location in 1997 similar to 2006 and 2015. Overall, it is very clear from the present results that it is possible to transport pollution from Indonesia to sub-tropical East Asia during extreme and higher-duration fire events like 1997, 2006, and 2015.

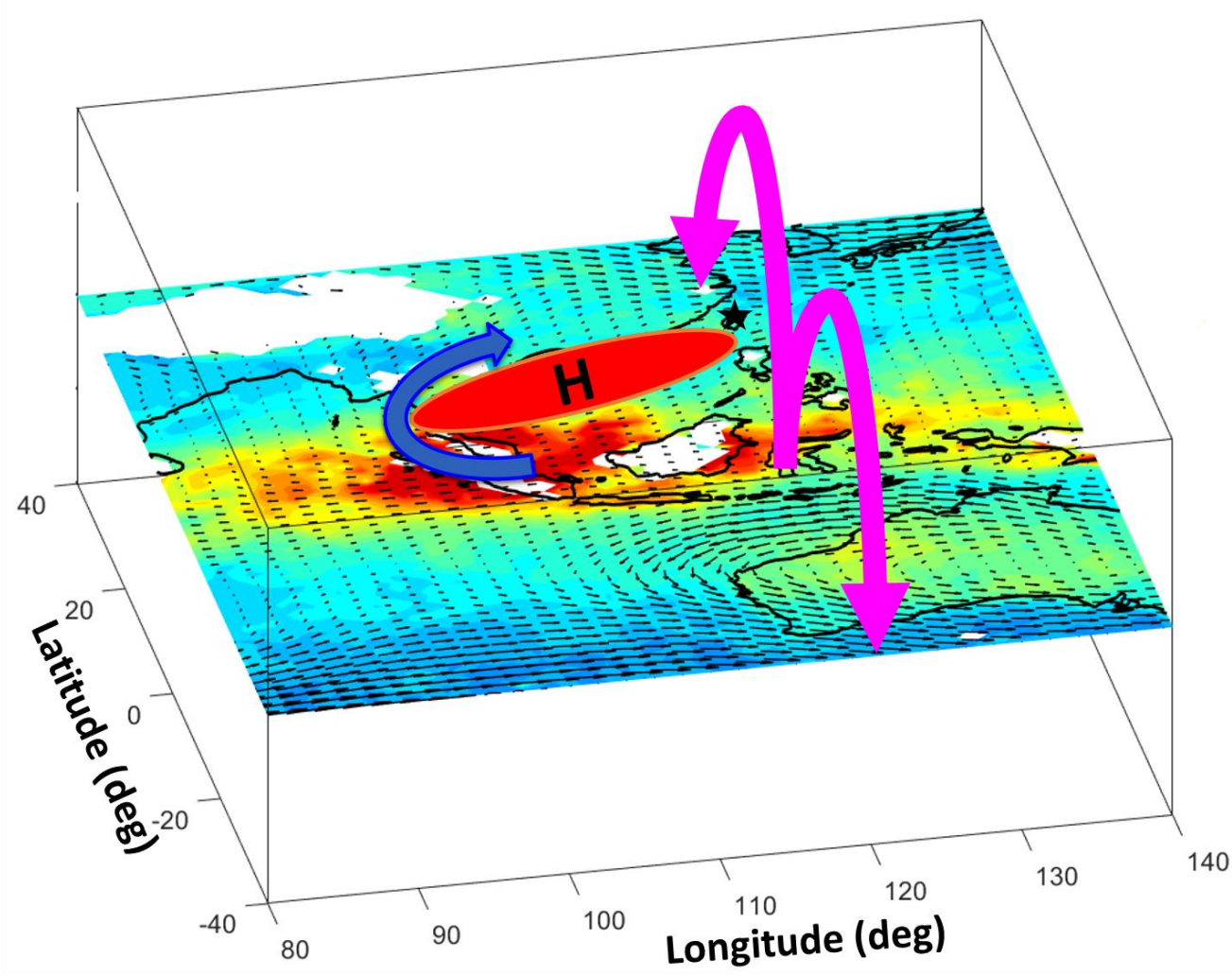

Figure 11. Schematic diagram of CO transport from Indonesian fires to subtropical East Asian region. The horizontal transport of CO due to the high-pressure anticyclone is denoted by the blue-colored arrow. H denotes a high-pressure anticyclone over northern parts of the South China Sea. Magenta-colored arrows indicate the transport of CO through the local Hadley circulation (over 110°–130°E). Black-colored star symbol represents the LABS location.

The major transport pathways of CO from Indonesia to subtropical East Asia are illustrated in a schematic diagram (Figure 11). Illustrated mechanisms include horizontal transport in the free troposphere due to El Niño and positive IOD-induced high-pressure anticyclone circulation, and vertical transport through the Hadley circulation. The southerlies on the southwest flank of the anticyclone merged with the subtropical westerlies over PSEA and then transported polluted air to LABS. Apart from this horizontal transport, CO was transported through the Hadley circulation to LABS in both events. However, there was a distinctly different Hadley Circulation strength in 2006 compared to 2015 due to the different El Niño conditions. These two events were strongly associated with positive IOD, but in 2006, the El Niño conditions were not well-developed, whereas in 2015 well-developed El Niño conditions were evident. These El Niño conditions further suppressed the HC over the western Pacific in 2015 compared to 2006. This suggested the importance of the background climate conditions (ENSO and IOD) on the pollutant transport process.

4. Summary and Conclusions

Due to the combined impact of positive phase IOD and El Niño-induced drought conditions in 2006 and 2015, Indonesia experienced extreme fire activity. MODIS active fire counts showed the largest fires in October 2006 and 2015 compared to the other years in the 16-year period in Indonesia. These record fires reflected two of the largest carbon emissions in the Indonesian region since 1997. Lulin Atmospheric Background Station (LABS, 23.47°N 120.87°E, 2862 m ASL) is the only high-altitude background station located in the western North Pacific region, and is optimally located to study some of these transport processes, including long-range transport of pollution in the free troposphere and stratospheric intrusions. Interestingly, during these two events (October 2006 and 2015), we noticed an abnormal enhancement of CO compared to other years at LABS from the in-situ measurements. In the present study, for the first time, the impact of Indonesia fire pollution on CO measurements at LABS and the plausible transport pathways for the transport of CO from Indonesia to sub-tropical East Asia were investigated. The main findings are summarized below:

1. Compared to 16-year (2006-2021) means, a substantial increase in CO mixing ratios of about ~47.2 ppb (37.2%) in October 2006 and ~36.7 ppb (28.9%) in October 2015 was observed at LABS.

2. By comparing the CO and atmospheric large-scale circulation data, we found two plausible transport pathways of CO from Indonesia to LABS. i.e. horizontal transport in the free troposphere and vertically through the Hadley Circulation.
3. El Niño and positive IOD-induced high-pressure anticyclone circulation over northern parts of the South China Sea play an important role in the horizontal transport of CO.
4. Distinct strength of the Hadley circulation over the western Pacific was observed in October 2006 (stronger) and 2015 (weaker). Well-developed El Niño conditions in October 2015 suppressed the strength of the Hadley Circulation over the western Pacific.

A changing warmer climate can influence carbon emissions and alter the transport pathways, hence impacting the various scales of air pollution and climate. Changes in the background climate will inevitably impact meteorological transport processes and the concentrations of pollutants arriving at downwind regions. Overall, the present results further provide knowledge to the atmospheric chemistry community about the different transport pathways of pollutants and the role of climate conditions.

Data availability

The CO data at LABS can be assessed at http://lulin.tw/index_en.htm. The AIRS and MOPITT CO data can be downloaded from the following websites https://disc.gsfc.nasa.gov/datasets/AIRS3STM_7.0 (AIRS project., 2019) and https://asdc.larc.nasa.gov/project/MOPITT. MERRA-2 data are available online through the NASA Goddard Earth Sciences Data Information Services Center (GES DISC; https://disc.gsfc.nasa.gov, last access: 30 May 2022). Nino 3.4 Index and IOD data can be downloaded through the following websites https://psl.noaa.gov/gcos_wgsp/Timeseries/Niño34/. https://psl.noaa.gov/gcos_wgsp/Timeseries/DMI/. The MODIS fire products can be downloaded from the following website https://firms.modaps.eosdis.nasa.gov/active_fire/.

Author contributions

Saginela Ravindra Babu: Conceptualization, Data curation, Formal analysis, Investigation, Software, Validation, Visualization, Writing – original draft preparation, Writing – review and editing; **Chang-Feng Ou-Yang**: Data curation, Software, Validation, Visualization; **Stephen M. Griffith**; Writing – review and editing; **Shantanu Kumar Pani**: Data curation and Visualization;

Steven S. Kong: Data curation and Visualization; **Neng-Huei Lin**: Conceptualization, Investigation, Funding Acquisition, Supervision, Resources, Writing – review and editing.

Competing Interest

The authors declare that they have no conflict of interest.

Acknowledgments

The work is primarily supported by the Ministry of Science and Technology, Taiwan under the grants of MOST 110-2811-M-008-562 and MOST 109-2811-M-008-553. Authors thanks to Taiwan Environmental Protection Administration (TEPA) for supporting the air pollutants monitoring at LABS. The authors thank NASA and NOAA for providing MOPITT, MODIS, and AIRS satellite data. We thank NASA's Global Monitoring and Assimilation Office (GMAO) for providing the Modern-Era Retrospective analysis for Research and Applications, Version 2 (MERRA-2) data. We also thank NOAA ESRL Physical Sciences Laboratory for providing Indian Ocean Dipole and Niño 3.4 index values through the following websites https://psl.noaa.gov/gcos_wgsp/Timeseries/DMI/ https://psl.noaa.gov/gcos_wgsp/Timeseries/Niño34/.

5. References

AIRS project (2019), Aqua/AIRS L3 Monthly Standard Physical Retrieval (AIRS-only) 1-degree x 1 degree V7.0, Greenbelt, MD, USA, Goddard Earth Sciences Data and Information Services Center (GES DISC), Accessed: (11 September 2022), 10.5067/UBENJB9D3T2H.

Bowman, K. P. and Cohen, P. J.: Interhemispheric exchange by seasonal modulation of the Hadley circulation, J. Atmos. Sci., 54, 2045–2059, https://doi.org/10.1175/1520-0469(1997)054%3C2045:IEBSMO%3E2.0.CO;2, 1997.

Bowman, K. P.: Transport of carbon monoxide from the tropics to the extratropics, J. Geophys. Res.-Atmos., 111, https://doi.org/10.1029/2005JD006137, 2006.

Chandra, S., Ziemke, J. R., Duncan, B. N., Diehl, T. L., Livesey, N. J. and Froidevaux, L.: Effects of the 2006 El Niño on tropospheric ozone and carbon monoxide: implications for dynamics and biomass burning, Atmos. Chem. Phys., 9, 4239–4249, https://doi.org/10.5194/acp-9-4239-2009, 2009.

462 Chandra, S., Ziemke, J. R., Schoeberl, M. R., Froidevaux, L., Read, W. G., Levelt, P.F. and
463 Bhartia, P. K.: Effects of the 2004 El Nino on tropospheric ozone and water vapor,
464 Geophys.Res. Lett., 34, L06802, https://doi.org/10.1029/2006GL028779, 2007.

465 Chi, K.H., Hung, N.T., Lin, C.Y., Wang, S.H., Ou-Yang, C.F., Lee, C.T. and Lin, N.H.: Evaluation
466 of Atmospheric PCDD/Fs at Two High-Altitude Stations in Vietnam and Taiwan during
467 Southeast Asia Biomass Burning. Aerosol Air Qual. Res. 16: 2706-2715.
468 https://doi.org/10.4209/aaqr.2015.11.0653, 2016.

469 Chuang, M. T., Fu, J. S., Lee, C. Te, Lin, N. H., Gao, Y., Wang, S. H., Sheu, G. R., Hsiao, T. C.,
470 Wang, J. L., Yen, M. C., Lin, T. H. and Thongboonchoo, N.: The simulation of long-range
471 transport of biomass burning plume and short-range transport of anthropogenic pollutants to a
472 mountain observatory in east Asia during the 7-SEAS/2010 Dongsha experiment, Aerosol Air
473 Qual. Res., 16(11), 2933–2949, https://doi.org/10.4209/aaqr.2015.07.0440, 2016.

474 Cheng, F.-Y., Yang, Z.-M., Ou-Yang, C.-F. and Ngan, F.: A numerical study of the dependence
475 of long-range transport of CO to a mountain station in Taiwan on synoptic weather patterns
476 during the Southeast Asia biomass-burning season, Atmos. Environ., 78, 277–290,
477 https://doi.org/10.1016/j.atmosenv.2013.03.020, 2013.

478 Cooper, O. R., Gao, R. S., Tarasick, D., Leblanc, T., and Sweeney, C.: Long-term ozone trends at
479 rural ozone monitoring sites across the United States, 1990–2010, J. Geophys. Res.-
480 Atmos.,117, 1990–2010, https://doi.org/10.1029/2012JD018261, 2012.

481 Deeter, M. N., Edwards, D. P., Francis, G. L., Gille, J. C., Mao, D., Martínez-Alonso, S., Worden,
482 H. M., Ziskin, D., and Andreae, M. O.: Radiance-based retrieval bias mitigation for the
483 MOPITT instrument: the version 8 product, Atmos. Meas. Tech., 12, 4561–4580,
484 https://doi.org/10.5194/amt-12-4561-2019, 2019.

485 Doherty, R. M., Stevenson, D. S., Johnson, C. E., Collins, W. J., and Sanderson, M. G.:
486 Tropospheric ozone and El Nino-Southern Oscillation: Influence of atmospheric dynamics,
487 biomass burning emissions, and future climate change, J. Geophys. Res., 111, D19304,
488 https://doi.org/10.1029/2005JD006849, 2006.

Duncan, B. N., Bey, I., Chin, M., Mickley, L. J., Fairlie, T. D., Martin, R. V., and Matsueda, H.: Indonesian wildfires of 1997: Impact on tropospheric chemistry, J. Geophys. Res., 108, 4458, https://doi.org/10.1029/2002JD003195, 2003a.

Duncan, B. N., Martin, R. V., Staudt, A., et al.: Inter-annual and seasonal variability of biomass burning emissions constrained by satellite observations, J. Geophys. Res., 108, 4100, https://doi.org/10.1029/2002JD002378, 2003b.

Field, R. D., van der Werf, G. R., and Shen, S. S. P.: Human amplification of drought-induced biomass burning in Indonesia since 1960, Nature Geoscience, 2, 185–188, https://doi.org/10.1038/ngeo443,2009.

Field, R. D., van der Werf, G. R., Fanin, T., Fetzer, E. J., Fuller, R., Jethva, H., Levy, R., Livesey, N. J., Luo, M., Torres, O., and Worden, H. M.: Indonesian fire activity and smoke pollution in 2015 show persistent nonlinear sensitivity to El Ni˜no-induced drought, Proceedings of the National Academy of Sciences, 113, 9204–9209, https://doi.org/10.1073/pnas.1524888113, 2016.

Gelaro, R., McCarty, W., Suárez, M. J., Todling, R., Molod, A., Takacs, L., Randles, C. A., Darmenov, A., Bosilovich, M. G., Reichle, R., Wargan, K., Coy, L., Cullather, R., Draper, C., Akella, S., Buchard, V., Conaty, A., Silva, A. M. da, Gu, W., Kim, G.-K., Koster, R., Lucchesi, R., Merkova, D., Nielsen, J. E., Partyka, G., Pawson, S., Putman, W., Rienecker, M., Schubert, S. D., Sienkiewicz, M., and Zhao, B.: The Modern-Era Retrospective Analysis for Research and Applications, Version 2 (MERRA-2), J. Climate, 30, 5419–5454, https://doi.org/10.1175/jcli-d-16-0758.1, 2017.

Giglio, L., Schroeder, W., and Justice, C. O.: The collection 6 MODIS active fire detection algorithm and fire products, Remote Sens. Environ., 178, 31–41, https://doi.org/10.1016/j.rse.2016.02.054, 2016.

Hadley, G.: Concerning the cause of the general trade-winds. Philos. Trans. R. Soc. Lond. 29, 58–62. https://doi.org/10.1098/rstl.1735.0014, 1735.

Heymann, J., Reuter, M., Buchwitz, M., Schneising, O., Bovensmann, H., Burrows, J. P., Massart, S., Kaiser, J. W., and Crisp, D.: CO2 emission of Indonesian fires in 2015 estimated from

satellite-derived atmospheric CO2 concentrations, Geophys. Res. Lett., 44, 1537–1544, https://doi.org/10.1002/2016gl072042, 2017.

Hsiao, T. C., Ye, W. C., Wang, S. H., Tsay, S. C., Chen, W. N., Lin, N. H., Lee, C. Te, Hung, H. M., Chuang, M. T., and Chantara, S.: Investigation of the CCN activity, BC and UVBC mass concentrations of biomass burning aerosols during the 2013 BASELInE campaign, Aerosol Air Qual. Res., 16, 2742–2756, https://doi.org/10.4209/aaqr.2015.07.0447, 2016.

Huang, L., Lin, W., Li, F., Wang, Y. and Jiang, B.: Climate Impacts of the Biomass Burning in Indochina on Atmospheric Conditions over Southern China. Aerosol Air Qual. Res. 19: 2707-2720. https://doi.org/10.4209/aaqr.2019.01.0028, 2019.

Huang, H. Y., Wang, S. H., Huang, W. X., Lin, N. H., Chuang, M. T., da Silva, A. M. and Peng, C. M.: Influence of Synoptic-Dynamic Meteorology on the Long-Range Transport of Indochina Biomass Burning Aerosols, J. Geophys. Res. Atmos., 125(3), https://doi.org/10.1029/2019JD031260, 2020.

Huijnen, V., Wooster, M. J., Kaiser, J. W., Gaveau, D. L. A., Flemming, J., Parrington, M., Inness, A., Murdiyarso, D., Main, B., and van Weele, M.: Fire carbon emissions over maritime southeast Asia in 2015 largest since 1997, Sci. Rep., 6, 26886, https://doi.org/10.1038/srep26886, 2016.

Lin, C.-Y., Hsu, H.-m., Lee, Y. H., Kuo, C. H., Sheng, Y.-F., and Chu, D. A.: A new transport mechanism of biomass burning from Indochina as identified by modeling studies, Atmos. Chem. Phys., 9, 7901–7911, https://doi.org/10.5194/acp-9-7901-2009, 2009.

Lin, N.-H., Tsay, S.-C., Maring, H. B., Yen, M.-C., Sheu, G.-R., Wang, S.-H., Chi, K. H., Chuang, M.-T., Ou-Yang, C.-F., Fu, J. S., Reid, J. S., Lee, C.-T., Wang, L.-C., Wang, J.-L., Hsu, C. N., Sayer, A. M., Holben, B. N., Chu, Y.-C., Nguyen, X. A., Sopajaree, K., Chen, S.-J., Cheng, M.-T., Tsuang, B.-J., Tsai, C.-J., Peng, C.-M., Schnell, R. C., Conway, T., Chang, C.-T., Lin, K.-S., Tsai, Y. I., Lee, W.-J., Chang, S.-C., Liu, J.-J., Chiang, W.-L., Huang, S.-J., Lin, T.-H. and Liu, G.-R.: An overview of regional experiments on biomass burning aerosols and related pollutants in Southeast Asia: From BASE-ASIA and the Dongsha Experiment to 7-SEAS, Atmos. Environ., 78, 1–19, https://doi.org/10.1016/j.atmosenv.2013.04.066, 2013.

Lin, C. C., Chen, W. N., Loftus, A. M., Lin, C. Y., Fu, Y. T., Peng, C. M. and Yen, M. C.: Influences of the long-range transport of biomass-burning pollutants on surface air quality during 7-SEAS field campaigns, Aerosol Air Qual. Res., 17(10), 2595–2607, https://doi.org/10.4209/aaqr.2017.08.0273, 2017.

Logan, J. A., Megretskaia, I., Nassar, R., Murray, L. T., Zhang, L., Bowman, K. W., Worden, H. M., and Luo, M.: Effects of the 2006 El Niño on tropospheric composition as revealed by data from the Tropospheric Emission Spectrometer (TES), Geophys. Res. Lett., 35, 1–5, https://doi.org/10.1029/2007GL031698, 2008.

Matsueda, H. and Inoue, H. Y.: Aircraft measurements of trace gases between Japan and Singapore in October of 1993, 1996, and 1997, Geophys. Res. Lett., 26, 2413–2416, https://doi.org/10.1029/1999GL900089, 1999.

Matsueda, H., Inoue, H. Y., and Ishii, M.: Aircraft observation of carbon dioxide at 8–13 km altitude over the western Pacific from 1993 to 1999, Tellus B, 54, 1–21, https://doi.org/10.1034/j.1600-0889.2002.00304.x, 2002.

Matsueda, H., Buchholz, R. R., Ishijima, K., Worden, H. M., Hammerling, D., and Machida, T.: Interannual Variation of Upper Tropospheric CO over the Western Pacific Linked with Indonesian Fires, SOLA, 15, 205–210, https://doi.org/10.2151/sola.2019-037, 2019.

Nara, H., Tanimoto, H., Nojiri, Y., Mukai, H., Zeng, J., Tohjima, Y., and Machida, T.: CO emissions from biomass burning in South-east Asia in the 2006 El Nino year: shipboard and AIRS satellite observations, Environ. Chem., 8, 213–223, https://doi.org/10.1071/EN10113, 2011.

Nassar, R., Logan, J. A., Megretskaia, I. A., Murray, L. T., Zhang, L., and Jones, D. B. A.: Analysis of tropical tropospheric ozone, carbon monoxide, and water vapor during the 2006 El Niño using TES observations and the GEOS Chem model, J. Geophys. Res.-Atmos., 114, D17304, https://doi.org/10.1029/2009JD011760, 2009.

Niwa, Y., Sawa, Y., Nara, H., Machida, T., Matsueda, H., Umezawa, T., Ito, A., Nakaoka, S.-I., Tanimoto, H., and Tohjima, Y.: Estimation of fire-induced carbon emissions from Equatorial

572 Asia in 2015 using in situ aircraft and ship observations, Atmos. Chem. Phys., 21, 9455–9473,
573 https://doi.org/10.5194/acp-21-9455-2021, 2021.

574 Ou-Yang, C. F., Lin, N. H., Lin, C. C., Wang, S. H., Sheu, G. R., Lee, C. Te, Schnell, R. C., Lang,
575 P. M., Kawasato, T. and Wang, J. L.: Characteristics of atmospheric carbon monoxide at a high-
576 mountain background station in East Asia, Atmos. Environ., 89, 613–622,
577 https://doi.org/10.1016/j.atmosenv.2014.02.060, 2014.

578 Ou-Yang, C. F., Ravindra Babu, S., Jia-Ren Lee, Ming-Cheng Yen, Stephen M. Griffith, Chia-
579 Ching Lin, Shuenn-Chin Chang and Neng-Huei Lin.: Detection of stratospheric intrusion events
580 and their role in ozone enhancement at a mountain background site in sub-tropical East Asia,
581 Atmos. Environ., 268, 118779, https://doi.org/10.1016/j.atmosenv.2021.118779, 2022.

582 Pani, S. K., Wang, S. H., Lin, N. H., Lee, C. Te, Tsay, S. C., Holben, B. N., Janjai, S., Hsiao, T.
583 C., Chuang, M. T. and Chantara, S.: Radiative effect of springtime biomass-burning aerosols
584 over northern Indochina during 7-SEAS/BASELInE 2013 campaign, Aerosol Air Qual. Res.,
585 16(11), 2802–2817, https://doi.org/10.4209/aaqr.2016.03.0130, 2016.

586 Pani, S. K., Ou-Yang, C.-F., Wang, S.-H., Ogren, J. A., Sheridan, P. J., Sheu, G.-R., and Lin, N.-
587 H. J. A. E.: Relationship between long-range transported atmospheric black carbon and carbon
588 monoxide at a high-altitude background station in East Asia, Atmos. Environ, 210, 86-99,
589 https://doi.org/10.1016/j.atmosenv.2019.04.053, 2019.

590 Pan, X., Chin, M., Ichoku, C. M., and Field, R. D.: Connecting Indonesian fires and drought with
591 the type of El Niño and phase of the Indian Ocean dipole during 1979–2016, J. Geophys. Res.-
592 Atmos., 123, 1–15, https://doi.org/10.1029/2018JD028402, 2018.

593 Park, S., Kim, S.W., Lin, N.H., Pani, S.K., Sheridan, P.J. and Andrews, E.: Variability of Aerosol
594 Optical Properties Observed at a Polluted Marine (Gosan, Korea) and a High-altitude Mountain
595 (Lulin, Taiwan) Site in the Asian Continental Outflow. Aerosol Air Qual. Res. 19: 1272-1283.
596 https://doi.org/10.4209/aaqr.2018.11.0416, 2019.

597 Parker, R. J., Boesch, H., Wooster, M. J., Moore, D. P., Webb, A. J., Gaveau, D., and Murdiyarso,
598 D.: Atmospheric CH4 and CO2 enhancements and biomass burning emission ratios derived

599 from satellite observations of the 2015 Indonesian fire plumes, Atmos. Chem. Phys., 16, 10111–
600 10131, https://doi.org/10.5194/acp-16-10111-2016, 2016.

601 Pochanart, P., Akimoto, H., Kajii, Y., and Sukasem, P.: Carbon monoxide, regional-scale, and
602 biomass burning in tropical continental Southeast Asia: Observations in rural Thailand, J.
603 Geophys. Res.-Atmos., 108, 4552, https://doi.org/10.1029/2002JD003360, 2003.

604 Ravindra Babu, S., VenkataRatnam, M., Basha, G., Liou, Y.-A., and Narendra Reddy, N.: Large
605 Anomalies in the Tropical Upper Troposphere Lower Stratosphere (UTLS) Trace Gases
606 Observed during the Extreme 2015–16 El Niño Event by Using Satellite Measurements,
607 Remote Sensing, 11, 687, https://doi.org/10.3390/rs11060687, 2019.

608 Ravindra Babu, S., Nguyen, L. S. P., Sheu, G.-R., Griffith, S. M., Pani, S. K., Huang, H.-Y., and
609 Lin, N.-H.: Long-range transport of La Soufrière volcanic plume to the western North Pacific:
610 Influence on atmospheric mercury and aerosol properties, Atmos. Environ., 268, 118806,
611 https://doi.org/10.1016/j.atmosenv.2021.118806, 2022.

612 Ravindra Babu, S., Pani, S.K., Ou-Yang, C.F., Lin, N.H.: Impact of 21 June 2020 Annular Solar
613 Eclipse on Meteorological Parameters, O3 and CO at a High Mountain Site in Taiwan. Aerosol
614 Air Qual. Res. 22, 220248. https://doi.org/10.4209/aaqr.220248, 2022.

615 Reid, J. S., Hyer, E. J., Johnson, R., Holben, B. N., Yokelson, R. J., Zhang, J., Campbell, J. R.,
616 Christopher, S. A., Di Girolamo , L., Giglio, L., Holz, R. E., Kearney, C., Miettinen, J., Reid,
617 E. A.,Turk, F. J., Wang, J., Xian, P., Zhao, G., Balasubramanian, R., Chew, B. N., Janai, S.,
618 Lagrosas, N., Lestari, P., Lin, N.-H., Mahmud, M., Nguyen, A. X., Norris, B., Oahn, N. T. K.,
619 Oo, M., Salinas, S. V., Welton, E. J., Liew, S. C.: Observing and understanding the Southeast
620 Asian aerosol system by remote sensing: An initial review and analysis for the Seven Southeast
621 Asian Studies (7SEAS) program, Atmos. Res., 122, 403-468,
622 https://doi.org/10.1016/j.atmosres.2012.06.005, 2013.

623 Sheu, G.-R., Lin, N.-H., Wang, J-L., Lee,C-T.; Lulin Atmospheric Background Station: A New
624 High-Elevation Baseline Station in Taiwan, J-STAGE, Volume 24, Issue 2, Pages 84-89,
625 https://doi.org/10.11203/jar.24.84, 2009.

626 Tsay, S. C., Maring, H. B., Lin, N. H., Buntoung, S., Chantara, S., Chuang, H. C., Gabriel, P. M.,
627 Goodloe, C. S., Holben, B. N., Hsiao, T. C., Christina Hsu, N., Janjai, S., Lau, W. K. M., Lee,
628 C. Te, Lee, J., Loftus, A. M., Nguyen, A. X., Nguyen, C. M., Pani, S. K., Pantina, P., Sayer, A.
629 M., Tao, W. K., Wang, S. H., Welton, E. J., Wiriya, W. and Yen, M. C.: Satellitesurface
630 perspectives of air quality and aerosol-cloud effects on the environment: An overview of 7-
631 SEAS/BASELInE, Aerosol Air Qual. Res., 16(11), 2581–2602,
632 https://doi.org/10.4209/aaqr.2016.08.0350 , 2016.

633 van der Werf, G. R., Dempewolf, J., Trigg, S. N., Randerson, J. T., Kasibhatla, P. S., Giglio, L.,
634 Murdiyarso, D., Peters, W., Morton, D. C., Collatz, G. J., Dolman, A. J., and DeFries, R. S.:
635 Climate regulation of fire emissions and deforestation in equatorial Asia, Proc. Natl. Acad. Sci.
636 USA, 105, 20350–20355, https://doi.org/10.1073/pnas.0803375105, 2008.

637 van der Werf, G. R., Randerson, J. T., Giglio, L., van Leeuwen, T. T., Chen, Y., Rogers, B. M.,
638 Mu, M., van Marle, M. J. E., Morton, D. C., Collatz, G. J., Yokelson, R. J., and Kasibhatla, P.
639 S.: Global fire emissions estimates during 1997–2016, Earth Syst. Sci. Data, 9, 697–720,
640 https://doi.org/10.5194/essd-9-697-2017, 2017.

641 Wang, C.: ENSO, Atlantic climate variability, and the Walker and Hadley circulations, in: The
642 Hadley circulation: Present, past and future, Springer, Berlin, 173–202,
643 https://doi.org/10.1007/978-1-4020-2944-8_7, 2004.

644 Wang, S.-H., Welton, E. J., Holben, B. N., Tsay, S.-C., Lin, N.-H., Giles, D., Stewart, S. A., Janjai,
645 S., Nguyen, X. A., Hsiao, T.-C., Chen, W.-N., Lin, T.-H., Buntoung, S., Chantara, S., and
646 Wiriya, W.: Vertical Distribution and Columnar Optical Properties of Springtime Biomass-
647 Burning Aerosols over Northern Indochina during 2014 7-SEAS Campaign, Aerosol Air Qual.
648 Res., 15, 2037–2050, https://doi.org/10.4209/aaqr.2015.05.0310, 2015.

649 Weng, H. Y., Behera, S. K., and Yamagata, T.: Anomalous winter climate conditions in the Pacific
650 rim during recent El Niño Modoki and El Niño events, Clim. Dynam., 32, 663–674,
651 https://doi.org/10.1007/s00382-008-0394-6, 2009.

652 Whitburn, S., Van Damme, M., Clarisse, L., Turquety, S., Clerbaux, C., and Coheur, P.-F.:
653 Doubling of annual ammonia emissions from the peat fires in Indonesia during the 2015 El
654 Niño, Geophys. Res. Lett., 43, 11007–11014, https://doi.org/10.1002/2016gl070620, 2016.

655 Worden, J., Jiang, Z., Jones, D. B. A., Alvarado, M., Bowman, K., Frankenberg, C., Kort, E. A.,
656 Kulawik, S. S., Lee, M., Liu, J., Payne, V., Wecht, K., and Worden, H.: El Niño, the 2006
657 Indonesian peat fires, and the distribution of atmospheric methane, Geophys. Res. Lett., 40,
658 4938–4943, https://doi.org/10.1002/grl.50937, 2013.

659 Yin, Y., Ciais, P., Chevallier, F., van der Werf, G. R., Fanin, T., Broquet, G., Boesch, H., Cozic,
660 A., Hauglustaine, D., Szopa, S., and Wang, Y.: Variability of fire carbon emissions in equatorial
661 Asia and its nonlinear sensitivity to El Niño, Geophys. Res. Lett., 43, 10472–10479,
662 https://doi.org/10.1002/2016gl070971, 2016.

663

664 **Table 1**. Detailed statistics of observed CO in October during 2006 to 2021 at LABS.

Year	Mean	Median	Standard Deviation	Change in CO (%)	Total data points
2006	**175.8**	**174**	**51**	**33.9**	**703**
2007	155.3	140	63.4	18.3	732
2008	125.5	125	26.9	-4.4	599
2009	127.1	125	35.5	-3.2	533
2010	143.9	136	38.1	9.6	739
2011	137.1	137	41.9	4.4	734
2012	155.8	153	39.4	18.7	643
2013	146.8	141	35.7	11.8	365
2014	125.6	120	39.8	-4.2	602
2015	**164.8**	**163.5**	**46.2**	**25.6**	**732**
2016	91.6	87	20.9	-30.2	732
2017	109.7	100.3	32.4	-16.4	744
2018	147.7	149.9	29.1	12.5	736
2019	142.4	142.8	37.7	8.5	742
2020	121.3	113.8	29.5	-7.5	742
2021	107.7	104.6	26.9	-17.9	744

665